



# Simulation Analysis of Industrial Plant Cyclone Dust Collection Systems for Air Quality Control

**Author:**

**Engr. Anacleto Cortez**

Program chair

Capiz State University- Main

Roxas City, Capiz.

**Alvin A. Lo-oc, CPM**

Student

## **Abstract**

This work simulated the optimization of cyclone separators, which are machines that separate particles from fluids. The balance between separation efficiency and pressure drop, two cyclone performance characteristics, is investigated. The former reflects the principal role of these devices, which is to segregate, whereas the latter evaluates their cost-effectiveness. The bulk of geometric parameter studies focus on the dimensions of the conical and cylindrical components, the dimensions and angles of the entry, the addition of additional pieces within the device, or the usage of a helical ceiling. For 3D modeling and simulation, the study employs AutoCad 202 and Ansys Fluent 2023. With a particle size of 10 microns, ash-solid is utilized as a dust alternative. The results reveal that a cyclone dust collector with two anti-venturi stages has much lower pressure and velocity than a single stage, resulting in less dust escape and more dust capture. The cyclone dust collector's efficiency can be boosted further by smoothening the design and adding more stages. To test the validity of these findings, additional study and simulation on this design using alternative software are needed.

## Introduction

Designers and researchers have been concerned with striking a proper balance between the two parameters that describe cyclone performance, namely separation efficiency and pressure drop, since the inception of cyclone separators. The former reflects the primary function of these devices, namely their ability to separate, whilst the latter assesses their cost-effectiveness. The majority of geometric parameter studies concentrate on the dimensions of the conical and cylindrical parts, the dimensions and angles of the entry, the addition of extra pieces inside the device, or the use of a helical ceiling. The most important research approaches for optimizing cyclone separators include experimental studies, the application of analytical models, Doppler and laser Doppler anemometry (PDA and LDA, respectively), particle image velocimetry (PIV), and computational fluid dynamics (CFD). Several turbulence models were used to simulate the flow inside a separator. Two-equation models, such as  $k$ - and  $k$ -RNG closures, have some drawbacks when modelling anisotropic flow. The Reynolds stress model (RSM) and large eddy simulation (LES) have been the most popular models in recent years. To increase the performance of cyclone separators, several researchers have used evolutionary algorithms and neural networks. The core group of cyclones was proposed by Stairmand, Lapple, and Swift, and their alterations are reliant on unique technological processes. These separators are circular-section cyclone separators. Square-section cyclones are another type that are used in the process of burning coal in circular fluidized bed (CFB) boilers. Initially, circular-section cyclone separators were used for this purpose, but they were found to have a number of issues over time, most notably their large size (due to their round shape) and the requirement for many layers of fireproof covering. These drawbacks increased the response time to temperature variations in the operating media caused by the variable working conditions of a CFB boiler, making integration of the boiler's operation with the separator difficult. As a result, academics began looking at possible remedies to this problem. In the 1990s, the Ahlstrom Corporation proposed a revolutionary design: a cyclone separator with a square cross-section (Pyroflow COMPACT). The design removed some of the drawbacks of circular cyclones used in conjunction with CFB boilers, was smaller in size than its round counterpart, could be coated with only a thin coating of fireproof cladding, and reduced the CFB installation's start and stop intervals. A benefit of round cyclones was the reduced pressure drop during the flow of the two-phase mixture through the separator. Unfortunately, this diminished separation efficiency, prompting further research towards

optimizing this technology. The next generation was a water-cooled square cyclone with a curved opening, which somewhat improved separation efficiency. Wang et al. (2019) created a temporary separation model after testing a square separator under high solid phase pressure. Su et al. studied the performance of a square cyclone with three different inlet configurations: regular, double, and downward-facing double.

### Related readings

The Philippine Clean Air Act of 1999 (RA8749)'s main objectives are to establish a comprehensive national program to combat air pollution that will be carried out by the government through efficient function and activity coordination and proper delegation of duties; encourage cooperation and self-regulation among citizens and industries through the use of incentives and market-based instruments; place a greater emphasis on pollution prevention than on control; and make provisions for. This also includes the creation of a financial or guarantee structure for clean-up, environmental rehabilitation, and restitution for individual damages.

To maintain sustainable operations and meet emission regulations and targets, the bulk of the manufacturing sector faces a substantial problem in dust control. It is possible to reduce dust emissions by either preventing emissions or by eliminating emissions of dust after they have occurred. The dust collection system's concept may seem simple, but if the design elements aren't thoroughly thought out, a lot can go wrong. Just a few of the engineering considerations that go into dust control systems include the efficient use of available space, the length of duct runs, the ease with which collected dust can be reintroduced into the process, the necessary electrical requirements, and the selection of the appropriate filter and control equipment.

Determining whether a centralized or decentralized system is better in the specific circumstance is another crucial decision. Important technical choices include identifying the problem, selecting the appropriate tools, and designing the best dust collection system for a given activity. In addition to considering dust as a potential contaminant, well-designed dust collection systems must also take into account the features of the system. Four components are necessary for a dust collecting system: an exhaust hood, ductwork, dust collector, and air mover/fan (Bhuiyan, Z. 2020).

In accordance with Presidential Decree No. 1151, issued on June 6, 1977, the Philippine Environmental Policy establishes a comprehensive and integrated national environmental protection program, primarily through the requirement of environmental impact assessments and statements, with the goal of advancing the positive and harmonious coexistence of nature and the Filipino people in the present and the future.

On June 11, 1978, Presidential Decree No. 1586 created the Philippine Environmental Effect Statement System (PEISS) as the national framework for all environmental effect assessment activities. According to the Philippine Environmental Policy (PD 1151) every development project is classified in the PEISS as either ecologically critical or environmentally non-critical. Every project that has the potential to harm the environment in any way must get an Environmental Compliance Certificate (ECC). These initiatives are regarded as crucial for the environment.

In light of the susceptibility of the Philippines and its people to climate change, Republic Act No. 9729: The Climate Change Act of 2009 integrates climate change adaptation and mitigation strategies into the policy formation and development efforts of all government agencies. It also established the Climate Change Commission, which is headed by the President of the Republic of the Philippines, as the focal point for all climate change-related actions and initiatives in the country.

## Related literature

According to Xiaochuan, L. et al. (2022) found that the dust-collecting pathways widened as K and V values increased. They also found that the bulk of dust-escape routes were restricted to the height between complete and local air curtains. As K rose, the increment rate slowed, and dust control effectiveness initially increased rapidly. For K = 1.5 and V = 5-6 m/s, dust control efficacy reached values of up to 95.54–96.27%.

Based on the results of numerical simulations, the prototype transshipment system for soybean clearance was developed, and smoke tracing tests were conducted to validate the effectiveness of air curtain dust control. Adoption of the developed system can significantly reduce occupational lung disease and boost clearing transshipment efficiency by around 67% (savings of about \$50,113 in terms of energy use and labor resources). An additional granary can be kept after using the newly developed method for 36.5-52.1 clearances.

While the average dust concentration rises and then decreases, and the MBFS dust removal performance is optimum at 90°, the average pressure drop of the WFDC rises and then declines as the inclination angle increases (30° to 150°). For total dust and respirable dust on-site in a coal preparation plant, the applied optimized WFDC outperformed the corresponding 91% and 88% dust suppression efficiencies (Hu S. Et al. 2023).

Two high-speed air curtains form at the shearer driver's operating position to effectively block the dust created by the coal cutting drum, and a trapezoidal full-section clean air chamber forms at the sidewalk. An air curtain with a 90 m<sup>3</sup>/min air volume provides the best dust management in this area while also cutting the diffusion distance of high concentration dust by 90 m. When this technology was applied in the field, the dust concentration in the shearer driver's working area was reduced to 79.23 mg/m<sup>3</sup>, and the dust control efficiency was 83%. It has been shown that the technique can reduce the amount of dust present throughout the tunnel, especially in the area where the shearer driver is working (Nie W. et al. 2023).

The dust suppression efficiency was 93% for dust with particles smaller than 75 μm and 95.2% for dust with particles between 180 and 250 μm when the water input into the dust collector was tuned at 1.0 m<sup>3</sup>/h at 1480 rpm. The field application in China's Tongqing Mine reduced the roadheader driver's exposure to respirable dust to 6.9 mg/m<sup>3</sup> with a 92.0% dust clearance rate. The wet-type swirl dust collector considerably improves dust collection efficiency and resolves the issue of nozzles and filter screens being easily blocked in underground excavation tunnels by conventional methods (Jin Z. et al. 2022).

As per Kun, Y. C., and Abdullah, A. Z. (2013) simulation can be used in place of actual stack measurement to predict dust emission and suggests that the minimum efficiency of a dust collector required for a boiler be determined. However, it is essential to regularly monitor the performance of the dust collector, which can be done by simultaneous isokinetic measurements at the intake and outlet of the dust collector, in order to correctly diagnose the issue and take appropriate remedial action.

The operation of boilers, fuel conditioning, performance evaluation, and reduction targets are only a few of the topics that have been covered. High dust emission will continue to cause major issues for the industry and environment if the aforementioned activities are not properly implemented and improved as needed.

According to Ho C. et al. (2021). The pulse dust collector's process design aims to bring down the price of filter components and reduced compressed air energy use, both of which are advantageous for the environment and the long-term growth of industrial sectors. The three optimal operating conditions are 10 s pulse interval time, 0.1 s pulse time, and less dust concentration. It has also been proven that energy savings can result in cheaper costs and a reduction in carbon emissions.

The choice of filter material, particle size, filtration speed, pulse-jet cleaning, nozzle size, nozzle distance, and other factors all affect the dust collector's air permeability in the simulation model. Future study will therefore use various dusts to numerically simulate the pressure drop caused by various transient powder cakes. Additionally, the current dust filter materials, like nanomaterial, will prevent pollution more effectively. However, pricing is a factor in how competitively businesses are positioned in the market. In order to precisely determine the ideal operating parameters and provide energy-saving solutions for industry as a reference, future research will continue to evaluate the scenario on-site with simulations and different types of filter material and climatic circumstances.

### Related Studies

Development that satisfies current demands without jeopardizing the ability of future generations to meet their own needs is known as sustainable development [13], and worldwide sustainable development is still advancing and spreading steadily [14]. Aside from that, sustainability has three other components, including cultural, social, and economic sustainability [15]. Environmental regulations on pollution prevention have changed from the end-of-pipe approach to front-end preventive control in order to achieve sustainable development [16]. The primary driver of global resource use and waste production is manufacturing. Nearly one-third of the world's energy use in 2004 came from the manufacturing sector, which had a 61% rise in energy consumption between 1971 and 2004 [17].

The manufacturing sector, on the other hand, has the potential to become a catalyst for the development of a sustainable society that can design and put into practice integrated sustainable practices and generate products and services to help improve environmental performance [18]. As a result, the idea of sustainable manufacturing was created. The manufacturing and service sectors can safeguard the environment, generate their own profits, satisfy customer needs, and give back to society by incorporating the spirit of sustainable development into their goods and services [19,20]. This will help them build a long-lasting business that is sustainable. Therefore, sustainable manufacturing fosters the use of new environmental technology while also promoting the reduction or elimination of production and processing waste through eco-efficient techniques [20].

There are an increasing number of studies on sustainable green manufacturing as a means of realizing sustainable manufacturing. The subjects cover such things as the rising cost of energy and resources, supplier risks, consumer demand, rules and legislation, lessening the impact on the environment, etc. [21]. Due to this, economic performance, environmental performance (ecological performance), and social performance are all crucial components of sustainable competitive advantage. Economic performance includes cost reduction, market share growth, profit margin increase, avoiding unnecessary environmental penalties, etc. Environmental performance (ecological performance) includes compliance with environmental regulations, controlling relevant pollution, recycling measures, etc.

Environmental performance is one of them that helps to boost economic performance. The ability to differentiate products, reach niche markets more easily, and promote pollution control technology are all benefits of improving environmental performance. Additionally, enhancing the environment's performance can save labor, material, and energy expenses [24].

A socially, environmentally, and economically sustainable globe is what is meant by "industrial sustainability," which is the final stage of a transformation process. Industrial sustainability undergoes a three-stage shift that includes adjustments to efficiency, technology, and system [25]. For process-related research on the use of natural resources by society and the effects of industrial activities, operation modifications and equipment design for less energy consumption are discussed, and new advancements in process planning and production scheduling that take environmental performance into account are highlighted [26,27].

As a result, there are basically three ways to lessen the influence of the manufacturing process on the environment: (22) Process improvement and optimization: the process is high-efficiency, low-cost, and environmental concerns are addressed. Development of new processes: To replace existing processes, new "green" processes are created. Process planning: Environmental integration aspects lean more toward sustainable production techniques and inventory control [28].

The four different types of dust collectors available today are cyclone, bag, electrostatic, and moist. There are three different types of bag-type dust collecting systems based on the cleaning technique: oscillation type, backwash air type, and pulse-jet type. In industrial processes, dust is frequently collected using the pulse dust collection method. The polluted air will pass through the filter and settle on its surface while the fan motor extracts the dust produced by the operation.

The process of using reverse high-pressure air to clean the filter element is typically used to regulate the cleaning time of the filter element. As a result, Equation (1) can be used to divide the pressure drop  $P_{Filter}$  caused by the dust collection filter into three pieces. The first is the pressure drop of the brand-new filter,  $P_f$ , which is specified by Darcy's law and has not yet filtered the dust. The second is referred to as the pressure drop of the temporary cake as  $P_c$  and is caused by the dust cake that forms on the surface of the filter element during filtering.

This section will modify to follow the pulse-jet air-cleaned dust cake. The third pressure drop is known as the pressure drop of the temporary powder cake as  $P_r$  and is brought on by dust particles entering the filter element and being unable to be cleaned and removed by pulse-jet air. This will steadily rise as the filter element is cleaned more frequently.

$$P_{Filter} = P_f + P_c + P_r$$

Darcy's law (1856) can be used to describe  $P_f$  to show the relationship between flow distance  $L_o$  and the pressure  $P_f$  in a fixed velocity  $V$  with a Reynolds number less than 2100, as shown in Equation (2), where  $\mu$  is the fluid's viscosity,  $K_f$  is the filter's permeability, and  $L_o$  is the filter's thickness.

$$P_f = \frac{1}{K_f} \times \mu L_o V$$

The production of temporary powder cake is the buildup of powder on the surface of the filter element over time in a stable flow with a Reynolds number less than 2100. The pressure drop of the temporary powder cake, denoted as  $P_c$ , will exhibit a linear connection between the mass and the applied pressure.

The Kozeny-Carman model, which is depicted as a collection of parallel capillaries or channels, was initially used to describe the pressure drop of a transient powder cake [29]. According to Equation (3), where  $d_s$  is the average diameter,  $K_{K-C}$  is the constant,  $\epsilon_0$  is the porosity of the filter elements, and  $C_{K-C}$  is the Cunningham slip correction factor, the total volume of the powder cake is equal to the void volume of the powder, and the surface area is equal to the surface area of the particles.

$$P_c = \left[ \frac{18}{d_s^2 \times C_{K-C}} \times \frac{2K_{K-C}(1 - \epsilon_0)}{\epsilon_0^3} \right] \times \mu L_o V$$

The porosity of the dust cake is equal to the ratio of the volume of the particles to the volume of the spherical shell according to the Happel cell model, which treats the powder cake as a collection of individual particles [20].

The dust mass  $W$  accumulated per unit area, as specified in Equation (13), can be calculated using the aforementioned formulae to convert the powder cake deposition thickness  $L_0$ , where  $C$  is the dust concentration and  $P$  is the dust density. According to Equation (14),  $P$  is made up of the filtration speed  $V$ , the mass of the powder cake  $W$ , and the resistance coefficient  $K_2$  of the powder cake.

$$L_0 = \frac{C}{\rho_p} \times \int V(t)dt = \frac{W}{\rho_p}$$

$$P_c = K_2 \times W \times V$$

Based on the Kozeny-Carman model, it takes into account the polydispersity dust particles and builds a  $K_2$  for the pressure drop of the temporary powder cake using the dynamic shape factor, mean diameter, and standard deviation, as shown in Equation (6). To get this function, the void function  $v(\epsilon_0)$  must be verified for the porosity of the dust cake.

$$K_2 = \frac{18\kappa}{d_g^2 \exp(4\ln^2 \sigma_g)} \frac{v(\epsilon_0)}{\epsilon_0^2} \times \frac{\mu}{\rho_p}$$

Because the dust in the filter can't be entirely eliminated, the filter will become blocked and its pressure drop will rise [30,31,32,33]. According to Equation (7), where  $SE$  is the resistance coefficient of the residual powder cake and  $V$  is the filtration rate, this pressure drop is consistently defined by the pressure drop of the residual powder cake as  $P_r$ , which will increase the number of pulse-jet cleanings [34,35,36].

$$P_r = SE \times V$$

The effectiveness of pulse cleaning, which can restore the filter element to a better initial state after cleaning and meet the goal of energy savings, was largely studied in the pertinent articles on the optimal operating parameters of dust collectors. The initial pressure of the storage tank, the average static pressure or the maximum pressure of the pulsed air acting on the surface of the filter, the size of the nozzle, the separation between the nozzle and the filter, the rate of filtration, and other factors were also studied in some of the experiments.

The cleaning effectiveness of the pulse-jet dust collection system can be evaluated by varying the operating parameters such as filtration speed, compressed air pressure, and nozzle diameter. The results revealed that the value of the compressed air is the primary factor that directly affects the pulse cleaning and that the pulse pressure on the filter bag will not always increase as the nozzle diameter increases [37]. The effect of filter material or folding filter form on cleaning effectiveness has been studied in detail. For instance, the filter with surface treatment is more effective in cleaning [38].

Additionally, it investigated the variations in pressure and acceleration in the filter bag using a variety of parameter studies, including the beginning tension of the filter bag, filter speed, compressed air pressure, pulse time, and nozzle shape. It was found that the cleaning effectiveness of the system improved with increasing pressure

and acceleration on the surface of the filter bag during pulse cleaning, and it was established that the compressed air pressure and nozzle shape are the primary factors affecting pulse cleaning [39].

Additionally, the effectiveness of cleaning in the pulse dust collector system under various cleaning modes is affected by the research of the wrinkle ratio of the folding filter [40]. In order to assess the filter's cleaning performance, the static pressure distribution on the surface must be analyzed. It shown that less static pressure on the filter's top will result in ineffective cleaning. Second, inadequate cleaning is more likely with folding filters due to their larger wrinkle ratio [41].

Additionally, the amount of leftover dust is utilized to assess the system's cleaning effectiveness. It examined the pulse peak pressure, filtration speed, filter size, and other variables and revealed that the pulse peak pressure plays a significant role in the system cleaning outcome. While the cleaning resistance brought on by the filtering speed has no effect on cleaning effectiveness when pressure is applied, the cleaning resistance increases with increasing filtering speed when peak pressure is insufficient. This is brought on by rising residual dust levels and poor cleaning performance [42].

The type of filter dust will also have a big impact on how well the dust collection system cleans [3]. In light of the foregoing, it should be noted that the impact of the pulse interval time  $T_w$ , pulse time  $T_p$ , and process dust concentration on the dust collector has not yet been covered.

The maintenance of equipment, the lowering of operating costs, and the increase of equipment reliability are all priorities for petrochemical enterprises. It is especially pertinent to dust collection systems currently in use [85,86,43,44,45,46,47,48,49], whose core elements are cyclones with relatively good performance, straightforward operation, and simple design. Their disadvantages include the relatively high hydraulic drag and walls that are vulnerable to abrasive wear [45,46,47,48]. As a result, cyclones for coarse and medium-degree gas filtration are frequently utilized in petrochemistry for production lines that convert C4-C5 paraffins to isoolefins using fluidized beds. These cyclones frequently modify the fractional size distribution of the catalyst due to particle crushing and abrasion when particles come into contact with the cyclone walls [49,50,51,52].

One of the most frequent issues with this type of cyclone is erosion, which usually affects the lower cone and higher input area. F. Fulchini [53] highlighted the gas dispensing nozzles, the bubbling layer, cyclones, and bending sections as the fluidized bed's high-stress regions where mechanical strain results in particle abrasion. Additionally, they recommended that since there are various abrasion mechanisms (surface abrasion, chipping, and fragmentation), each of these abrasion sources be examined separately.

The predominant mechanism is caused by a confluence of particle characteristics, operating conditions, and device geometry [54,55,56,57]. J. Valuer and J. One of the most important causes of particle abrasion, especially at high surface gas flow rates, according to Reppenhagen [58], is the cyclone. J. In the context of surface particle abrasion for catalyst particles in fluid catalytic cracking (FCC), Werther et al.'s model of particle abrasion caused by cyclones was put forth [59].

According to an examination of the data, the abrasion rate was influenced by the characteristics of the material, the kinetic energy of the gas, and the particle size. J. In order to evaluate the model's dependability, Reppenhagen et al. [60] examined nine distinct cyclone geometries. They used a model that only considered abrasion, whereas J. In particular, for new catalysts, Werther et al. [61] noted that particles would experience intense chipping and/or fragmentation if the inlet flow rate was increased and/or particle loading was decreased.

At a specific loading of solid particles, the hydrodynamics of a cyclone—which controls particle speed and residence time—and the physical characteristics of particles—which influence the relationship between abrasive wear and operating conditions—are factors that contribute to abrasive wear in the cyclone [62,63]. In these research, numerical modeling was carried out utilizing the CFD-DEM technique while accounting for particle dynamics.



In cyclone separators, the gas flow is frequently highly turbulent and unstable. To improve cyclone performance, many researchers have investigated various geometric and operating factors using computational approaches [64,65,66,67,68].

The Reynolds stress turbulence model (RSM) was advised by A.J. Hoekstra et al. [69] after using three turbulence models to examine air flows inside a cyclone with three distinct swirl numbers. M.D. By simulating a gas flow inside the cyclone using the RSM turbulence model, Slack et al. [70] found that the numerical results and the experimental laser Doppler anemometry (LDA) measurements were in good agreement.

Gronald, G., and J.J. Derksen [71] used the large eddy simulation (LES) method and the two-equation RANS turbulence model to simulate the air flow inside the cyclone, and he then compared the CFD results to the experimental results acquired using LDA. They demonstrated that for predicting varying flow rates, the LES model outperformed the RANS model. However, because the LES model needs high-fidelity grids, calculations are time-consuming.

Numerous scholars have underlined that another significant issue with the numerical modeling of flow in cyclones is the need to take into account geometric considerations. R.M. Alexander [72] investigated a few geometrical factors that affect cyclone performance. J. The impact of cone tip diameter on pressure drop and cyclone performance was examined by Gimbut et al. [73].

The issue of increased catalyst consumption as a result of cyclone crushing and abrasion is systemic in nature. The geometrical characteristics of the apparatus, which result in the production of specific gas-dynamic flow structures affecting the particle-wall interaction, are the most important factors for cyclones. The CFD-DEM model is currently used in the majority of research to numerically simulate the gas dynamics and particle motion in cyclones [55,74,75,76,77], allowing one to forecast cyclone efficiency, hydraulic drag, etc. at various operating parameters [78,79,80,81]. However, it should be noted that little is known about erosive wear of the cyclone internal surface.

Generally speaking, centrifugal cyclones are the high-performance, dependable machinery that makes it possible to effectively remove fine particles from the gas medium. This type of cyclone, however, exhibits low wear resistance and is vulnerable to cyclone wall erosion [82,83]. Therefore, creating unique separators with reduced erosive wear can be an industry-useful answer. The most promising separating tool is an arc-shaped element separator (SAE) [84]. The presence of specially created arc-shaped pieces in SAE, which create non-cyclonic flows, is a benefit. Investigating erosion in the innovative gadget makes sense from both a fundamental and applied standpoint.

Their research compared the cyclone and proposed separator with arc-shaped elements for separating solid catalyst particles from gases in order to compare erosive wear and highlight the unique separator's separation characteristics.

The proposed dust collector allows for a 6.5-fold reduction in erosive wear for identical operating modes and operating parameters (temperature, pressure, particle size and speed, etc.) when separating catalyst particles from the gas using two devices (a cyclone and a separator with arc-shaped elements). The organized wave-like flow structure in the new separator results in particles being propelled into distinct SAE parts with a greater intensity during eddy formation, which reduces the equipment-damaging side processes, resulting in lesser erosive wear compared to that in a cyclone.

The SAE differs from conventional centrifugal separators in that it generates higher-intensity centrifugal forces. As the gas travels around the arc-shaped elements, several locations of eddy formation with relatively tiny eddy radii develop, improving pararticle separation from gas flows.

It has been shown that for both examined devices, the wall erosion rate increases with increasing average catalyst particle size (>40 m). Since larger particles are coarser and more likely to collide chaotically with the device

body during settling, wall erosion can now be seen in both the upper and lower cylindrical parts of the cyclone, as opposed to just the upper part of the cyclone when particles are as small as 40  $\mu$ m.

The first two rows of elements in the separation device with arc-shaped elements are most prone to degradation. The construction of the dust-filled medium in the device's front half hasn't fully formed, which is what's causing this. Particles enter the identical zones within the first two rows of the arc-shaped elements as a result of rectilinear and inertial motion. Arc-shaped parts in the suggested separator experience erosive wear, limiting the development of holes in the device body and catalyst loss.

The cyclone and separator with arc-shaped parts contain functions that demonstrate the relationship between erosive wear rate and particle diameter; using these functions, one can forecast how long the devices will last. Regarding the foreseeable future, it is suggested that the separator with arc-shaped elements be used in petrochemical facilities, particularly in processes like fluidized-bed dehydrogenation of C4-C5 isoparaffins to isoolefins (Salakhova E. et al. 2023).

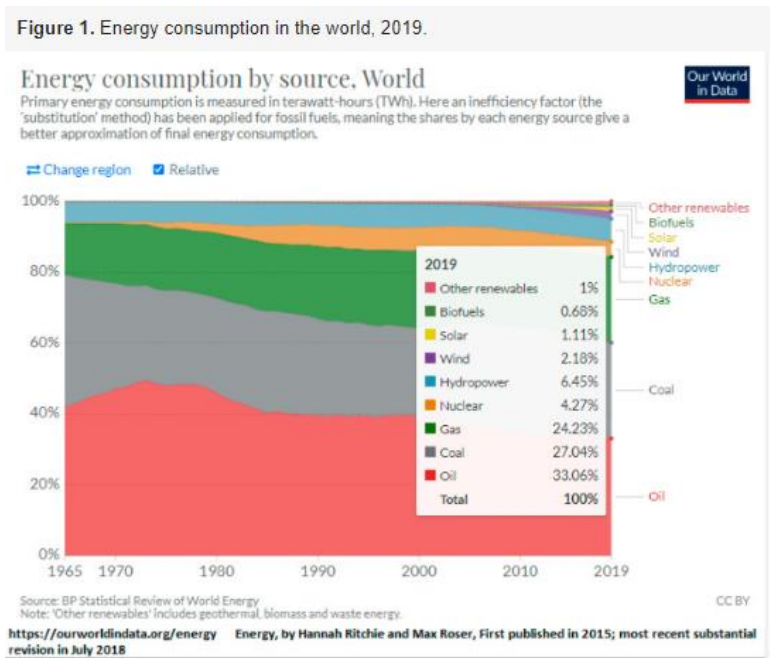
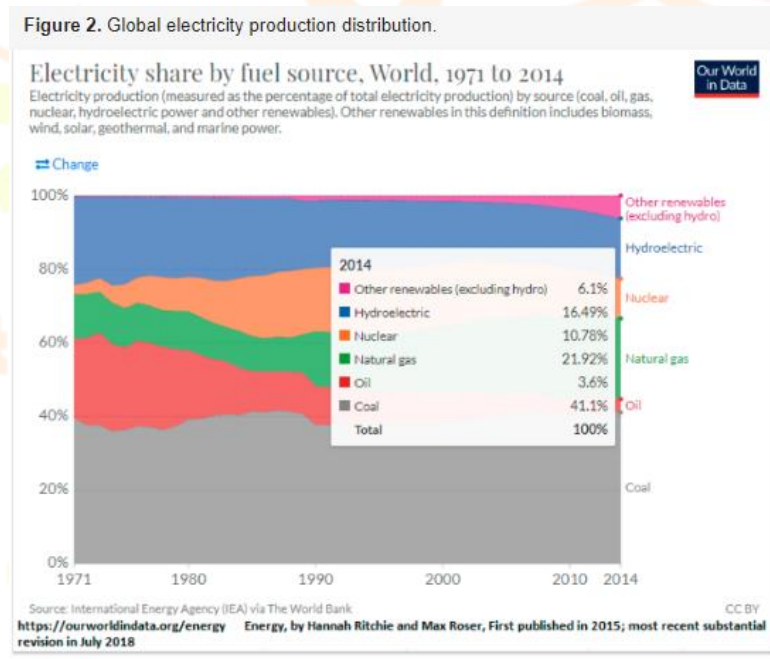
According to the Energy Information Administration of the US Department of Energy [88,89], and summarized in Table 1, the industrial sector consumes 32.53% of the overall energy consumption worldwide.

With such a high proportion, it not only represents the electricity consumption but also makes it highly justifiable to work toward improving the energy efficiency of industrial applications. In regions where energy production produces large concentrations of greenhouse gases (GHG), these initiatives should be addressed.

Additionally, a comprehensive study on energy usage [90] included data on energy consumption and the production of electricity worldwide broken down by source. Figures 1 and 2 show that 67.03% of the world's power is produced by fossil fuels, and that as of 2019, fossil fuel usage accounts for 84.33% of all energy consumption worldwide.

**Table 1.** Energy consumption by sector, 2019 [1].

Sector	Petawatt-Hours	Percentage
Residential	20.98	20.98
Commercial	17.94	17.94
Industrial	95.75	32.53
Transportation	84.02	28.55
Total	272.43	100

**Figure 1.** Energy consumption in the world, 2019.**Figure 2.** Global electricity production distribution.

The attempts to optimize industrial energy consumptions through more accurate management systems are more than justified by these high percentages and the pressing need to reduce our GHG emissions. As the effects of climate change are seen more widely, other incentives become more urgent. According to Bunsen [91], these take the shape of laws like taxes, subsidies, tradeable emission permits, and green certificates.

One way to increase an industrial system's energy efficiency is to better manage its energy use by tailoring it to the demands of production. The amount of electrical energy used in industrial systems directly affects the operational costs.

Numerous industrial applications use more energy than is necessary to meet demand. One can think of compressed air and dust collection systems, which virtually usually have leaks [92]. During the manufacturing times, these systems frequently operate at full capacity.

This consumption surplus may appear minor when viewed in terms of individual industrial systems, but it increases significantly when viewed in terms of the entire factory and all of its systems. The advantages can only grow if a control technique makes it possible to close the gap between input and output.

Energy is used by industrial systems to control the strain placed on them and to run processes that raise the value of the input resources. If an interest is shown in the effectiveness of the system, it is vital to monitor and alter the energy levels required to carry out these tasks because they frequently change over time.

The system itself and its operational characteristics must therefore be stressed in the first section of an efficiency analysis, utilizing carefully chosen performance indicators. This decision should be based on the parameters that will be optimized, and a benchmarking method should be given top priority. In their study [91], Bunse et al. (2011) studied the energy efficiency indicators and benchmarking methodologies by putting together a summary of the state of the science and the unmet requirements in the field. In order to maximize the energy efficiency of industrial systems, it is clear that more sophisticated control strategies must be developed.

To be able to decide what parameters will help to efficiently monitor the system's functioning and adapt to the load imposed on it, an overview of the system's design and physical configuration must be examined. An approach from a textbook, such as the one suggested in Modeling and Analysis of Dynamic Systems [93], can be used to determine the parameters and machine variables. It is important to understand the physics underlying the system's implicated operations since doing so will enable optimization techniques to be used.

The investigation of the indicated physical phenomena will serve as the foundation for any necessary modeling developments. Any industrial system's optimization process should ultimately aim for better and more accurate controlling strategies in order to increase energy efficiency.

The ideal solution needs to be modified for the industrial system under investigation, whether it be using soft controls, hard controls, as defined by Naidu and Rieger [94,95], or a combination of the two. A comprehensive examination of the system should be done before deciding on the precise type of control to use. This study must be done taking into account the unique characteristics of the system, the different technologies, and the physics suggested in its design. By simulating the system's reaction to changes made for energy efficiency, a modeling strategy can prove to be a useful tool for the analysis and design of the control strategy.

The accuracy and usefulness of the data taken into account for the best modifications is one of the primary issues when creating an adaptive control system. The obvious objective in the case of dust collectors is to adjust the energy output of the source to only use the appropriate amount of energy at all times. The difficult part is determining the actual load placed on the dust collector's electric motor as a foundation for the system's power consumption changes.

The velocities of the air flow in the ducts, which are directly related to the differential pressures present in the different parts of the system, are the important parameters for appropriate dust collection. The amount of dust in the ducts, its size and shape, as well as the flow's temperature and humidity, are other factors that may affect the system's performance [96, 97].

According to Clarke's study [9], sawdust particles with moisture contents ranging from 8% to 82% had fluidization velocities that differ by 0.16 m/s, which seems to have little impact. The void percentage between particles has an effect on the fluidization velocities, according to Kunii's Fluidization Engineering manual [97]. For fine particles, this crucial flow parameter rises by up to 8% at temperatures up to 500 °C, but it has no effect on coarse particles, such include sawdust particles. Compared to the other stated parameters, these final two have a substantially lesser impact on the system's performance.

According to Leith's cyclone performance study [98], the optimization of the cyclone performance depends on the sizes and shapes of the dust particles as well as the solid phase densities. The efficiency is expressed in the cyclone efficiency curves as the ratio of the weight of particles of a given size that are collected to the weight of those particles entering the cyclone. As a result, it provides the cyclone's separation efficiency for particular particle sizes. It is obvious to draw the conclusion that efficiency rises as particle size does.

The velocity of the flow at the cyclone's entrance, which is managed by varying the speed of the electric motor driving the fan, continues to be the most important factor in determining optimal separation. Since it will be the main adjustment parameter of this analysis, it is important to confirm its effect on the overall efficiency of the cyclone. As the inlet gas velocity rises, the pressure drop rises as well. Both an empirical and a numerical solution yielded these curves. The substance was a common raw ingredient for cement. The typical particle diameter and density employed were 29.9  $\mu\text{m}$  and 3320  $\text{kg/m}^3$ , respectively.

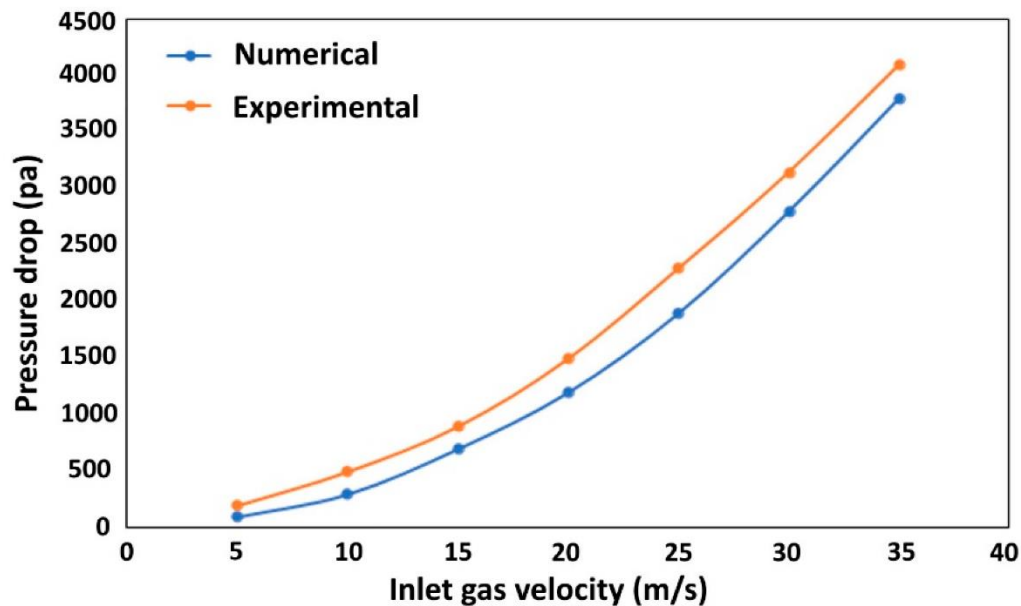


Figure 3. The influence of the inlet velocities on the pressure drop in the cyclone.

Huang A. et al. (2018) [99]. has also researched and modelled it. a cyclone's hydrodynamics and separation capacities are impacted by an increase in dust density. From their simulations and testing, they were able to establish that when the density of the particle phase of the flow grows, the pressure drop and tangential velocity in the cyclone would decrease and the separation efficiency will increase.

This is explained by the presence of larger particles, which have a sweeping effect on the smaller particles and cause them to concentrate more along the cyclone's wall region, where separation efficiency is higher. The control approach that will be designed must take into account this relationship.

The separating capacities of the cyclone therefore bear the brunt of the impacts of fluctuations in pressure drops on its overall performance. According to Wang et al. (2021), the pressure drop is influenced by both the flow's input velocity and the separation efficiency of the cyclone. As seen in the chart of Figure 4, this impact was also supported by Huang A. et al. [99] and other writers (Shepherd and Lapple, Coker 2015).

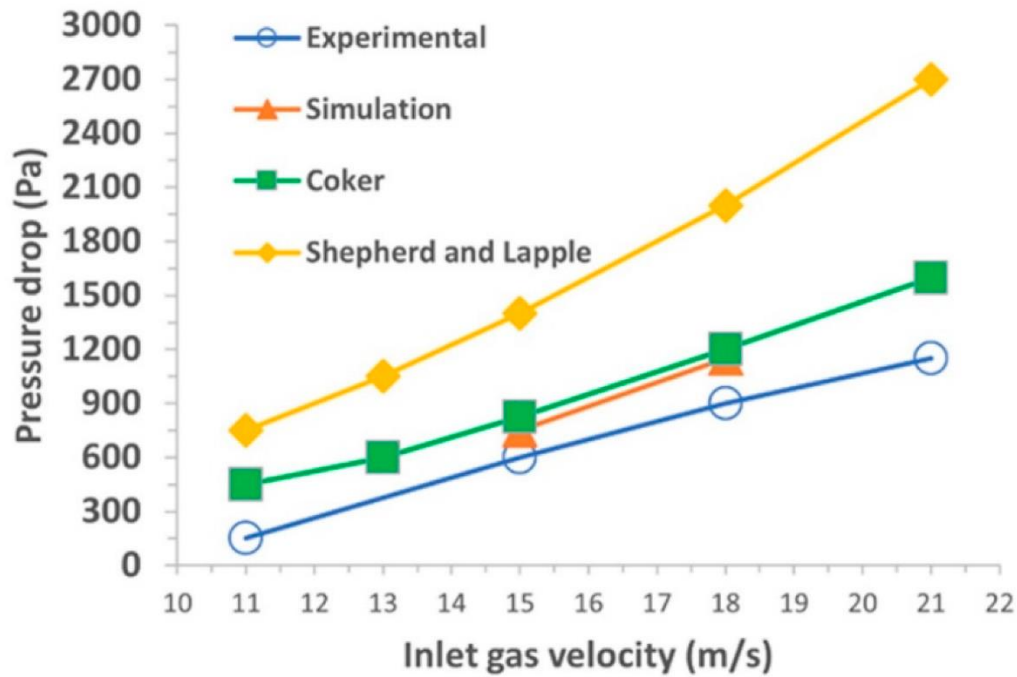


Figure 4. Comparisons of pressure drops.

The fluidization of solid particles in a gas flow along a network of pipe packed with solids at one or more cross-sections is known as dense phase pneumatic conveying. The fluidized dense phase and the plug-type dense phase have been recognized as two different forms of dense phase transport circumstances. The idea of pneumatic conveying is used in numerous industrial applications, for instance dust collection systems.

It is generally accepted in the literature study that the ideal arrangement for pneumatic conveying will depend on how the particles move through the pipes. It is noted that dense phase transport is more effective.

The next phase in dust collection system optimization is determining the size and form of the particles that will be transported (Geldart D., Molerus O. and Pan R.). this greatly influenced the outcome. To further understand the impact of these criteria, Jones and Williams created a comparison table.

The calculating methods can be evaluated based on the flow pattern and particle properties to choose the one that is most appropriate for the given issue. Therefore, the multiphase flow velocities and the pressure differentials [100], which depend on the velocities, are the main factors influencing the dust collection systems. They are based on the characteristics of the moving fluid and the moving particles. The model that can be used to develop a control strategy that can effectively adjust the system's power consumption, and thus permit operation cost savings and environmental benefits, depending on the energy production method of the systems operation region, is further driven by the determination of the relationship between these two fundamental parameters.

The achievement of the major objective put forth, i.e., the energy efficiency of industrial systems, would result from further advancements in control procedures that take into account the criteria described by this literature review. According to Bunse [91], extensive research must be conducted on energy efficiency and its monitoring. A future publication from the authors of this work will be presented, summarizing some of the recommendations of Bunse [101] Beaulac P. et al. (2022), and one can refer to the article to acknowledge all the research areas that have still to be studied.

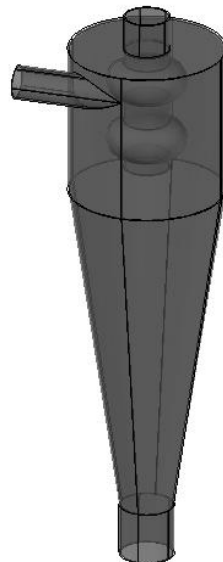
According to Zhang, J., Liang, D., & Cao, Y. (2023). the more symmetrical the distribution of tangential velocity field and static pressure field is, the greater the cyclone dust collector's dust removal efficiency is, the more stable the flow field is, and the lower the turbulence intensity is. Furthermore, the center cyclone's growing speed is

adversely connected with dust removal effectiveness. As a result, an antiventuri cyclone dust collector with a scrambling column was designed. When the inlet air speed is 6 m/s, the dust removal efficiency of the improved device is 97.0%, which is 5.1% higher than that of the original device, and when the inlet air speed is 8 m/s, the dust removal efficiency of the improved device is 97.3%, which is 4.16% higher than that of the original device. With the increase of the inlet air speed, the difference between them keeps decreasing.

### Methodology

This paper uses AutoCad 202 for the 3D model of the cyclone dust collector and Ansys fluent 2023 for simulation of the air and dust inside the cyclone dust collector. Instead of actual dust the designer uses ash-solid because it is the closest material to a dust available, the size used for ash-solid is 10 microns, the mesh was tetrahedron, mesh element size is 0.01 mm, gravity of  $9.81 \text{ m/s}^2$ , energy equation, k-epsilon, K-epsilon model was RNG- swirl Dominated flow, interaction with continuous phase, update DPM sources Every Flow Inter Action, 323.15 K, DPM-reflec, pressure- velocity coupling scheme “SIMPLE” and “ second order upwind”, standard initialization, 1000 iteration, Computational Fluid Dynamics or CFD method, SIMPLE calculation and the inlet velocity is 10m/s, inlet pipe diameter is 30 mm, depth of exhaust pipe if 225 mm, diameter of the exhaust is 75 mm, diameter of dust outlet is 90 mm, total height is 960 mm. The designer uses 2 antiventuri for the exhaust pipe.

### Design figure



### Results and discussion

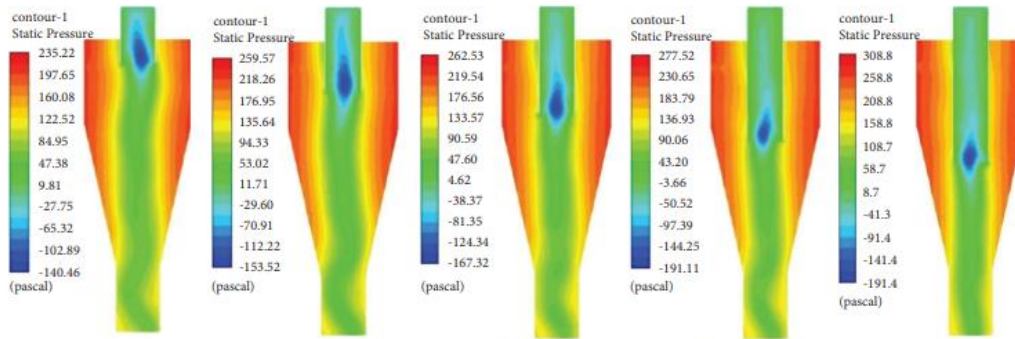


FIGURE 5: Static pressure cloud of an exhaust pipe with the depth of 75 mm, 150 mm, 225 mm, 300 mm, and 375 mm.

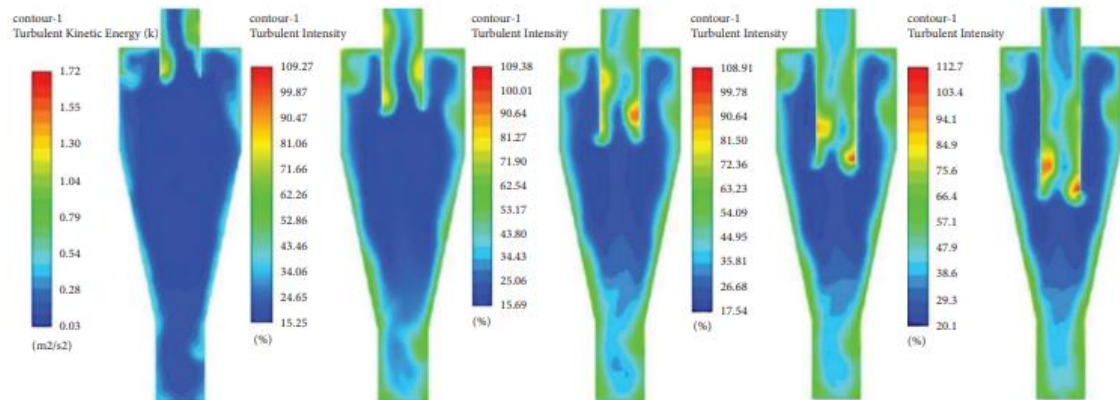
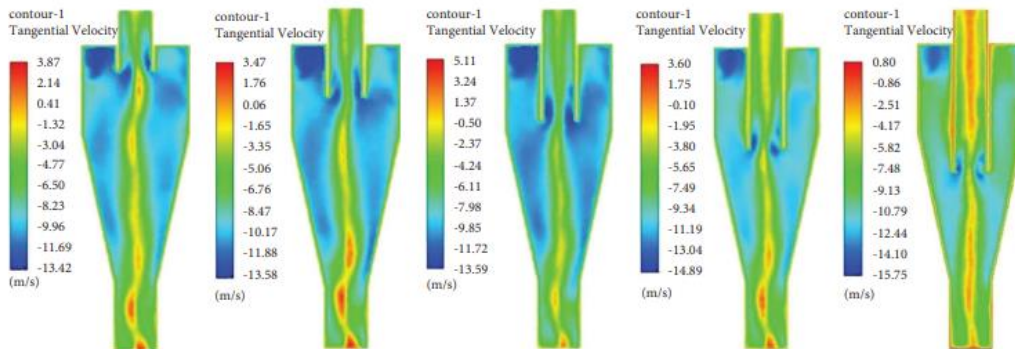
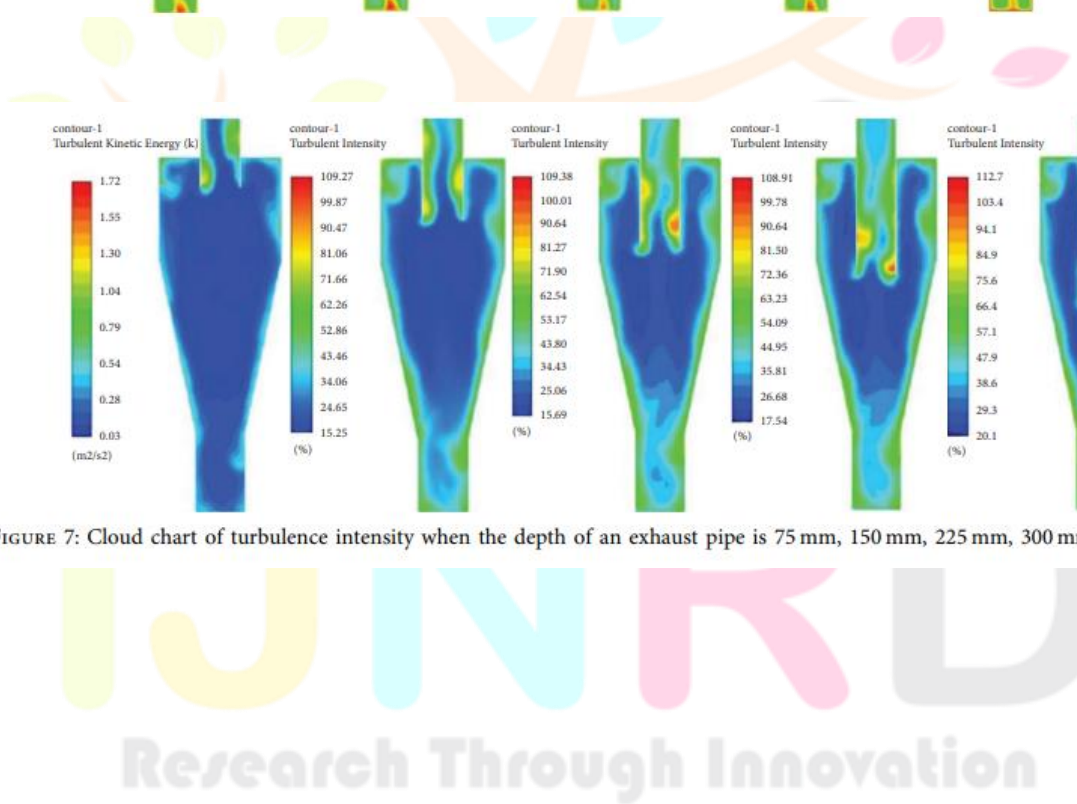
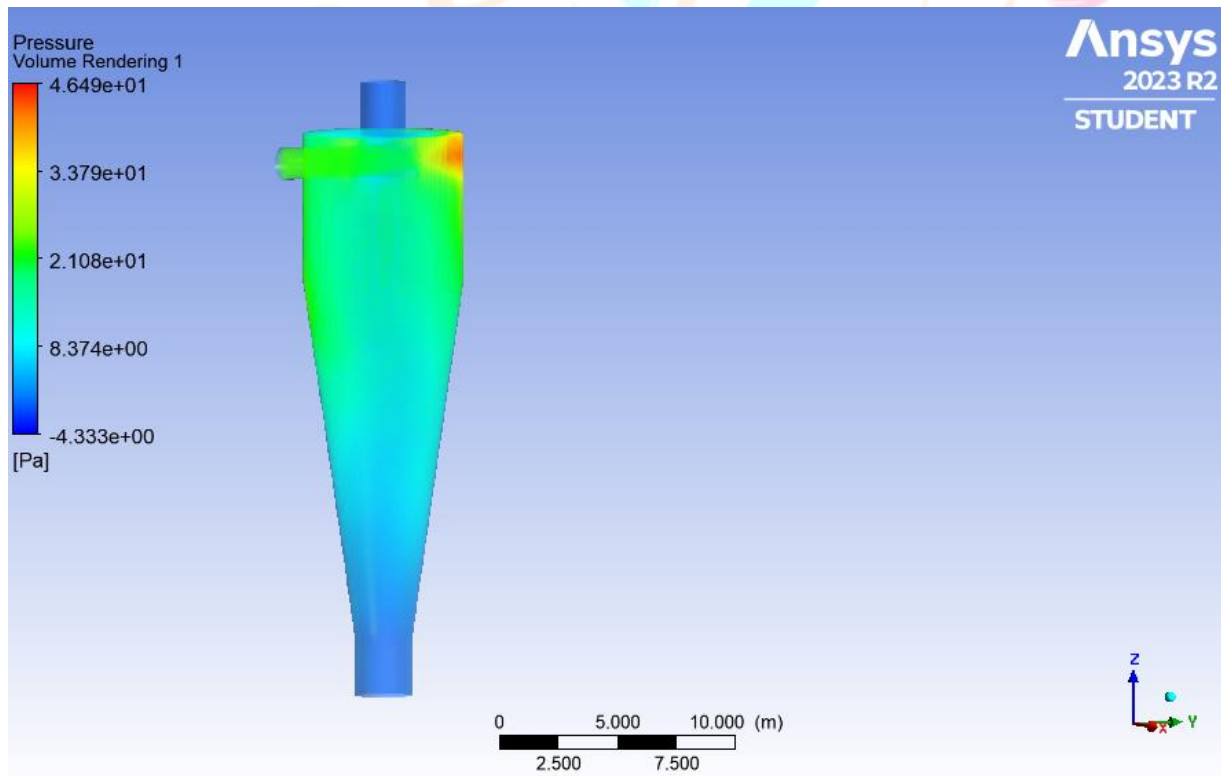
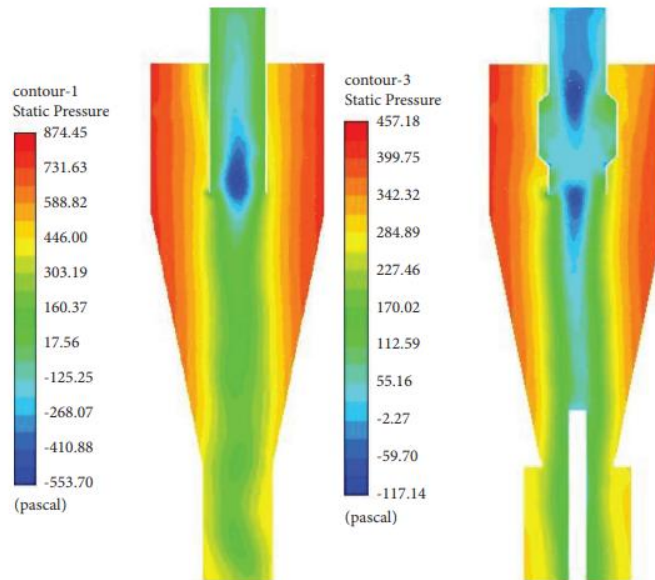


FIGURE 7: Cloud chart of turbulence intensity when the depth of an exhaust pipe is 75 mm, 150 mm, 225 mm, 300 mm, and 375 mm.







Research Through Innovation

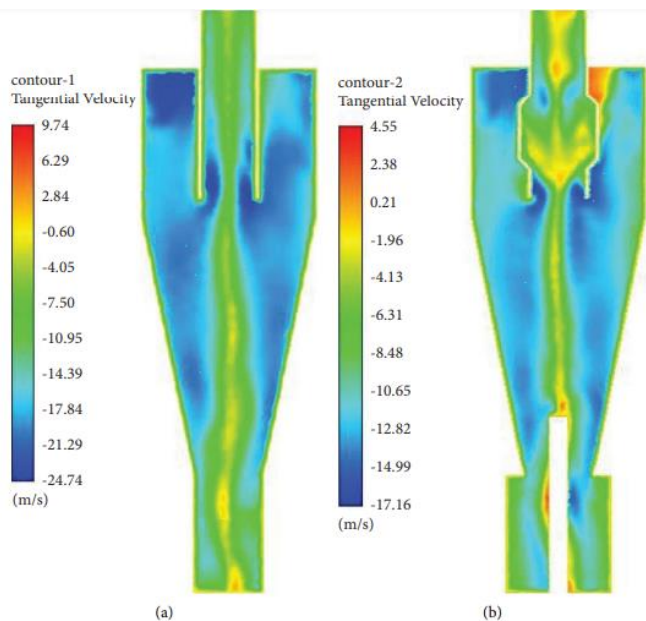


FIGURE 10: Tangential velocity distribution. (a) Original device. (b) Improved device.

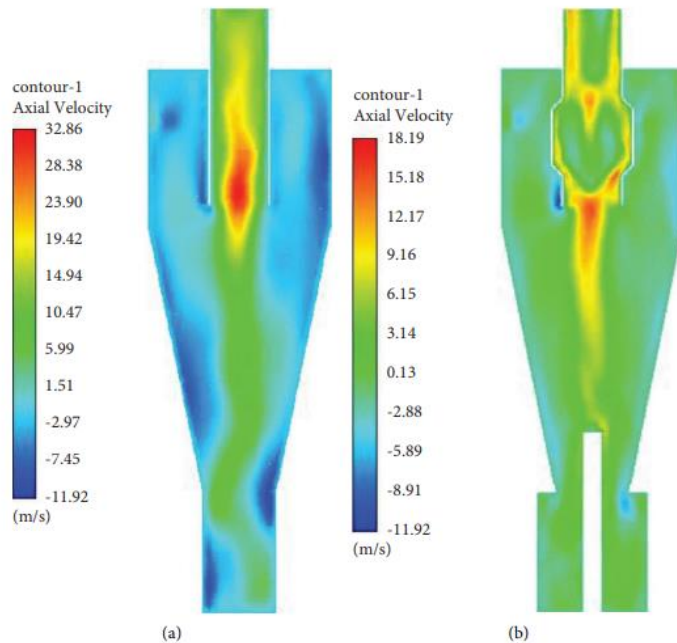
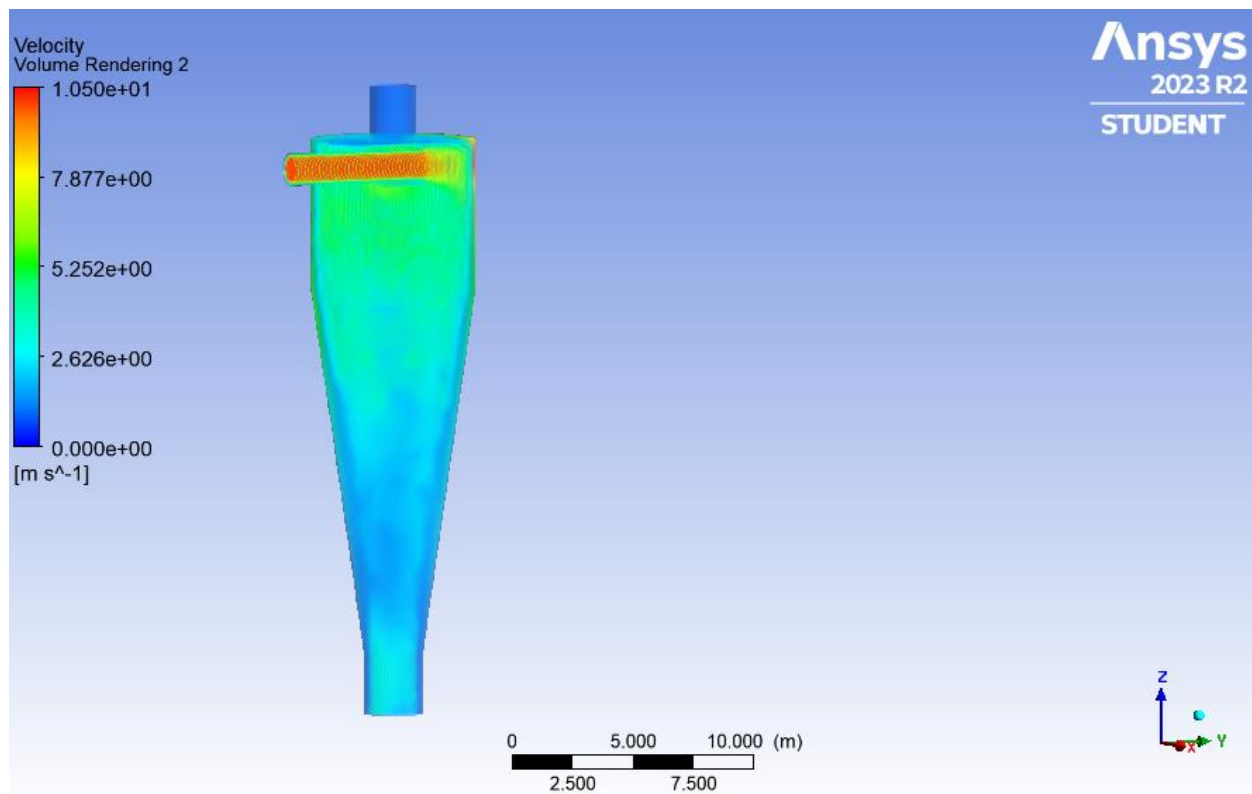


FIGURE 11: Axial velocity distribution. (a) Original device. (b) Improved device.

Research Through Innovation



Based on the results from Ansys Fluent 2023, the maximum pressure of the cyclone dust collector with 2 stages antiventuri wa  $4.649e+01$  or 46.49 Pascal. This result is significantly lower than a single stage antiventuri, also the maximum velocity of the 2 stages antiventuri cyclone dust collector is  $1.050e+01$  or 10.5 /s which is also significantly smaller than a single stage i.e 18.19 m/s. Because of the significant pressure and velocity drop the amount of dust the escape through the exhause pipe is greatly minimize and the amount of dust the goes to the dust collection bag is greater or equal to 99%. Therefor the number of stages of antiventuri meter will increase the efficiency of the cyclone dust collector and circular antiventuri is better than a rectangular antiventuri design.

### Conclusion

Antiventuri design was a great method to increase the efficiency of a cyclone dust collector. You could also increase the efficiency of the antiventuri effect by smoothing the design and add number of stages.

## Recommendation

The designer encourages further research and simulation on this design using different software to test the validity of this papers claim. The designer also recommends to test different types and sizes of dust as well as inlet velocity and the volumes of each sections.

## References

1. R.A. 8749. (n.d.). [https://lawphil.net/statutes/repacts/ra1999/ra\\_8749\\_1999.html](https://lawphil.net/statutes/repacts/ra1999/ra_8749_1999.html)
2. Bhuiyan, Z. (2020). Design analysis of Dust collection system. ResearchGate. [https://www.researchgate.net/publication/338541015\\_Design\\_analysis\\_of\\_Dust\\_collection\\_system](https://www.researchgate.net/publication/338541015_Design_analysis_of_Dust_collection_system)
3. Bhuiyan, Z. (2019). Dust Collection Systems. ResearchGate. [https://www.researchgate.net/publication/342452550\\_Dust\\_Collection\\_Systems](https://www.researchgate.net/publication/342452550_Dust_Collection_Systems)
4. Presidential Decree No. 1151, s. 1977 | GOVPH. (1977, June 6). Official Gazette of the Republic of the Philippines. <https://mirror.officialgazette.gov.ph/1977/06/06/presidential-decree-no-1151-s-1977/>
5. Joselito Guianan Chan, Managing Partner, Chan Robles and Associates Law Firm. (n.d.). PHILIPPINE ENVIRONMENT LAWS - CHAN ROBLES VIRTUAL LAW LIBRARY. <https://chanrobles.com/pd1586.htm#PD1586>
6. Republic Act No. 9729 | GOVPH. (2009, October 23). Official Gazette of the Republic of the Philippines. <https://www.officialgazette.gov.ph/2009/10/23/republic-act-no-9729/>
7. Xiaochuan, L., Mingrui, Z., YeFeng, J., Li, W., Xinli, Z., Xi, C., Haoyu, B., & Xianming, D. (2022). Air curtain dust-collecting technology: Investigation of factors affecting dust control performance of air curtains in the developed transshipment system for soybean clearance based on numerical simulation. Powder Technology, 396, 59–67. <https://doi.org/10.1016/j.powtec.2021.10.018>
8. Hu, S., Li, S., Cheng, H., Jin, H., Hou, J., Gui, C., Chen, X., Yuan, L., & Zhou, F. (2023). Study on the Wet Dust Collection Mechanism of Metal-Based Filter Screens and the Effect of Its Inclination Angle on Dust Removal Performance. Chemical Engineering Research & Design, 176, 430–437. <https://doi.org/10.1016/j.psep.2023.06.036>
9. Nie, W., Zhang, Y., Lidian, G., Zhang, X., Peng, H., & Chen, D. (2023). Research on airborne air curtain dust control technology and air volume optimization. Chemical Engineering Research & Design, 172, 113–123. <https://doi.org/10.1016/j.psep.2023.01.073>
10. Jin, Z., Hu, S., Zhu, X., Feng, G., & Sun, J. (2022). Research on wet-type swirl dust collection technology and its application in underground excavation tunnels. Advanced Powder Technology, 33(12), 103851. <https://doi.org/10.1016/j.appt.2022.103851>
11. Kun, Y. C., & Abdullah, A. Z. (2013). Simulation of total dust emission from palm oil mills in Malaysia using biomass fuel composition and dust collector efficiency models. SpringerLink, 4(1), 19. <https://doi.org/10.1186/2251-6832-4-19>
12. Ho, C., Tang, Y., & Chiu, W. (2021). The Optimal Performance of the Energy Efficiency of a Pulse Dust Collection System towards Sustainability. Applied Sciences, 11(22), 10941. <https://doi.org/10.3390/app112210941>
13. World Commission on Environment and Development (WCED). Our Common Future; Oxford University Press: Oxford, UK, 1987. [Google Scholar]

14. AL-ALwani, M. *Towards Sustainable Middle Eastern Cities: A Local Sustainability Assessment Framework*; School of Architecture, Design, and Environment, University of Plymouth: Plymouth, UK, 2014. <https://pearl.plymouth.ac.uk/bitstream/handle/10026.1/3010/2014al-alwani10242513phd.pdf>
15. Kong, L. Improbable art: The creative economy and sustainable cluster development in a Hong Kong industrial district. *Eurasian Geogr. Econ.* **2013**, *53*, 182–196. [[Google Scholar](#)] [[CrossRef](#)]
16. Kengpol, A.; Boonkanit, P. The decision support Framework for developing ecodesign at conceptual phase based upon ISO/TR 14062. *Int. J. Prod. Econ.* **2011**, *131*, 4–14. [[Google Scholar](#)] [[CrossRef](#)]
17. OECD. *Sustainable Manufacturing and Eco-Innovation: Framework, Practices and Measurement*; OECD: Paris, France, 2009. [[Google Scholar](#)]
18. Maxwell, D.; Sheate, W.; Van Der Vorst, R. Functional and systems aspects of the sustainable product and service development approach for Industry. *J. Clean. Prod.* **2006**, *14*, 1466–1479. [[Google Scholar](#)] [[CrossRef](#)]
19. Gond, J.; Grubnic, S.; Herzig, C.; Moon, J. Configuring management control systems: Theorizing the integration of strategy and sustainability. *Manag. Account. Res.* **2012**, *23*, 205–223. [[Google Scholar](#)] [[CrossRef](#)] [[Green Version](#)]
20. Carrillo-Hermosilla, J.; del Rio, P.; Konnola, T. Diversity of eco-innovations: Reflections from selected case studies. *J. Clean. Prod.* **2010**, *18*, 1073–1083. [[Google Scholar](#)] [[CrossRef](#)]
21. Reich-Weiser, C.; Vijayaraghavan, A.; Dornfeld, D. Appropriate use of green manufacturing frameworks. In Proceedings of the CIRP Life Cycle Engineering Conference, Hefei, China, 19–21 May 2010. [[Google Scholar](#)]
22. Bureau of Energy. The Annual Energy Outlook in Energy-Saving and Carbon-Reduction Services of Manufacturing Industries 2018, Ministry of Economic Affairs in Taiwan. Available online: <https://www.moeaboe.gov.tw/ECW/populace/home/Home.aspx> (accessed on 8 November 2021).
23. Tan, J.; Zailani, S. Green value chain in the context of sustainability development and sustainable competitive advantage. *Glob. J. Environ. Res.* **2009**, *3*, 234–245. [[Google Scholar](#)]
24. Ambec, S.; Lanoie, P. Does it pay to be green: A systematic overview. *Acad. Manag. Perspect.* **2008**, *22*, 45–62. [[Google Scholar](#)]
25. Tonelli, F.; Evans, S.; Taticchi, P. Industrial sustainability: Challenges, perspectives, actions. *Int. J. Bus. Innov. Res.* **2013**, *7*, 143–163. [[Google Scholar](#)] [[CrossRef](#)]
26. Sutherland, J.W.; Skerlos, S.J.; Haapala, K.R.; Cooper, D.; Zhao, F.; Huang, A. Industrial sustainability: Reviewing the past and envisioning the future. *J. Manuf. Sci. Eng.* **2020**, *142*, 110806. [[Google Scholar](#)] [[CrossRef](#)]
27. Arena, M.; Ciceri, N.D.; Terzi, S.; Bengo, I.; Azzone, G.; Garetti, M. A state-of-the-art of industrial sustainability: Definitions, tools and metrics. *Int. J. Prod. Lifecycle Manag.* **2009**, *4*, 207–251. [[Google Scholar](#)] [[CrossRef](#)]
28. Ramani, K.; Ramanujan, D.; Bernstein, W.Z.; Zhao, F.; Sutherland, J.; Handwerker, C.; Choi, J.K.; Kim, H.; Thurston, D. Integrated sustainable life cycle design: A review. *J. Mech. Des.* **2010**, *132*, 091004. [[Google Scholar](#)] [[CrossRef](#)] [[Green Version](#)]
29. Chen, Z.; Bao, B.; Zhu, W.; Lin, Z. Effect of test dust on performance test for a pleated filter cartridge. *Aerosol Air Qual. Res.* **2015**, *15*, 2436–2444. [[Google Scholar](#)] [[CrossRef](#)] [[Green Version](#)]
30. Li, S.; Wang, F.; Xin, J.; Xie, B.; Hu, S.; Jin, H. Study on effects of particle size and maximum pressure drop on the filtration and pulse-jet cleaning performance of pleated cartridge filter. *Process Saf. Environ. Prot.* **2019**, *123*, 99–104. [[Google Scholar](#)] [[CrossRef](#)]
31. Choi, J.H.; Ha, S.J.; Bak, Y.C.; Park, Y.O. Particle size effect on the filtration drag of fly ash from a coal power plant. *Korean J. Chem. Eng.* **2002**, *19*, 1085–1090. [[Google Scholar](#)] [[CrossRef](#)]
32. Saleem, M.; Krammer, G. On the stability of pulse-jet regenerated-bag. *Chem. Eng. Technol.* **2012**, *35*, 877–884. [[Google Scholar](#)] [[CrossRef](#)]
33. Li, J.; Li, S.; Zhou, F. Effect of cone installation in a pleated filter cartridge during pulse-jet cleaning. *Powder Technol.* **2015**, *284*, 245–252. [[Google Scholar](#)] [[CrossRef](#)]

34. Park, B.; Kim, S.; Jo, Y.; Lee, M.H. Filtration characteristics of fine particulate matters in a PTFE/Glass composite bag filter. *Aerosol Air Qual. Res.* **2012**, *12*, 1030–1036. [[Google Scholar](#)] [[CrossRef](#)] [[Green Version](#)]
35. Li, J.; Zhou, F.; Li, S. Experimental study on the dust filtration performance with participation of water mist. *Process Saf. Environ. Prot.* **2017**, *109*, 357–364. [[Google Scholar](#)] [[CrossRef](#)]
36. Tanabe, E.; Barros, P.; Rodrigues, K.; Aguiar, M. Experimental investigation of deposition and removal of particles during gas filtration with various fabric filters. *Sep. Purif. Technol.* **2011**, *80*, 187–195. [[Google Scholar](#)] [[CrossRef](#)]
37. Lu, H.C.; Tsai, C.J. Influence of different cleaning conditions on cleaning performance of pilot-Scale pulse-jet Baghouse. *J. Environ. Eng.* **2003**, *129*, 811–818. [[Google Scholar](#)] [[CrossRef](#)] [[Green Version](#)]
38. Calle, S.; Contal, P.; Thomas, D.; Bemer, D.; Leclerc, D. Evolutions of efficiency and pressure drop of filter media during clogging and cleaning cycles. *Powder Technol.* **2002**, *128*, 213–217. [[Google Scholar](#)] [[CrossRef](#)]
39. Simon, X.; Thomas, D.; Bémer, S.D.; Calle, S.; Régnier, R.; Contal, P. Influence of cleaning parameters on pulse-jet filter bags performances. *Filtration* **2004**, *4*, 253–260. [[Google Scholar](#)]
40. Lo, L.M.; Chen, D.R.; Pui, D. Experimental study of pleated fabric cartridges in a pulse-jet cleaned dust collector. *Powder Technol.* **2010**, *197*, 141–149. [[Google Scholar](#)] [[CrossRef](#)]
41. Lo, L.M.; Hu, S.C.; Chen, D.R.; Pui, D. Numerical study of pleated fabric cartridges during pulse-jet cleaning. *Powder Technol.* **2010**, *198*, 75–81. [[Google Scholar](#)] [[CrossRef](#)]
42. Li, Q.; Zhang, M.; Qian, Y.; Geng, F.; Song, J.; Chen, H. The relationship between peak pressure and residual dust of a pulse-jet cartridge filter. *Powder Technol.* **2015**, *283*, 302–307. [[Google Scholar](#)] [[CrossRef](#)]
43. Fu, P.; Zhu, J.; Li, Q.; Cheng, T.; Zhang, F.; Huang, Y.; Ma, L.; Xiu, G.; Wang, H. DPM simulation of particle revolution and high-speed self-rotation in different pre-self-rotation cyclones. *Powder Technol.* **2021**, *394*, 290–299. [[Google Scholar](#)] [[CrossRef](#)]
44. Yu, G.; Dong, S.; Yang, L.; Yan, D.; Dong, K.; Wei, Y.; Wang, B. Experimental and numerical studies on a new double-stage tandem nesting cyclone. *Chem. Eng. Sci.* **2021**, *236*, 1–14. [[Google Scholar](#)] [[CrossRef](#)]
45. Farzad, P.; Seyyed, H.H.; Khairy, E.; Goodarz, A. Numerical investigation of effects of inner cone on flow field, performance and erosion rate of cyclone separators. *Sep. Purif. Technol.* **2018**, *201*, 223–237. [[Google Scholar](#)]
46. Celis, G.E.O.; Loureiro, J.B.R.; Lage, P.L.C.; Freire, A.P.S. The effects of swirl vanes and a vortex stabilizer on the dynamic flow field in a cyclonic separator. *Chem. Eng. Sci.* **2022**, *248*, 1–45. [[Google Scholar](#)] [[CrossRef](#)]
47. Haig, C.W.; Hursthouse, A.; Mcilwain, S.; Sykes, D. An empirical investigation into the influence of pressure drop on particle behaviour in small scale reverse-flow cyclones. *Powder Technol.* **2015**, *275*, 172–181. [[Google Scholar](#)] [[CrossRef](#)]
48. Haake, J.; Oggian, T.; Utzig, J.; Rosa, L.M.; Meier, H.F. Investigation of the pressure drop increase in a square free-vortex cyclonic separator operating at low particle concentration. *Powder Technol.* **2020**, *374*, 1–21. [[Google Scholar](#)] [[CrossRef](#)]
49. Zhang, Y.; Jiang, Y.; Xin, R.; Yu, G.; Jin, R.; Dong, K.; Wang, B. Effect of particle hydrophilicity on the separation performance of a novel cyclone. *Sep. Purif. Technol.* **2020**, *237*, 1–11. [[Google Scholar](#)] [[CrossRef](#)]
50. Chang, Y.-L.; Jiang, X.; Li, J.-P.; Fu, P.-B.; Yuan, W.; Xin, R.-K.; Huang, Y.; Wang, H.-L. Inlet particle-sorting cyclones configured along a spiral channel for the enhancement of PM<sub>2.5</sub> separation. *Sep. Purif. Technol.* **2021**, *257*, 1–13. [[Google Scholar](#)] [[CrossRef](#)]
51. Seyed Masoud, V.; Farzad, P.; Kamali, M.; Jebeli, H.J. Numerical Investigation of the Impact of Inlet Channel Numbers on the Flow Pattern, Performance, and Erosion of Gas-particle Cyclone. *Chem. Eng. Iran. J. Oil Gas Sci. Technol.* **2018**, *7*, 59–78. [[Google Scholar](#)]
52. Basaran, M.; Erpul, G.; Uzun, O.; Gabriels, D. Comparative efficiency testing for a newly designed cyclone type sediment trap for wind erosion measurements. *Geomorphology* **2011**, *130*, 343–351. [[Google Scholar](#)] [[CrossRef](#)]

53. Fulchini, F. Particle Attrition in Circulating Fluidised Bed Systems. Ph.D. Dissertation, University of Leeds, Leeds, UK, 2020; p. 298. [[Google Scholar](#)]
54. Welt, J.; Lee, W.; Krambeck, F.J. Catalyst attrition and deactivation in fluid catalytic cracking system. *Chem. Eng. Sci.* **1977**, *32*, 1211–1218. [[Google Scholar](#)] [[CrossRef](#)]
55. Fu, P.; Yu, H.; Li, Q.; Cheng, T.; Zhang, F.; Huang, Y.; Lv, W.; Xiu, G.; Wang, H. CFD-DEM simulation of particle revolution and high-speed self-rotation in cyclones with different structural and operating parameters. *Chem. Eng. J. Adv.* **2021**, *8*, 1–13. [[Google Scholar](#)] [[CrossRef](#)]
56. Li, Q.; Wang, J.; Xu, W.; Zhang, M. Investigation on separation performance and structural optimization of a two-stage series cyclone using CPFD and RSM. *Adv. Powder Technol.* **2020**, *31*, 3706–3714. [[Google Scholar](#)] [[CrossRef](#)]
57. Azri, M.; Nor, M.; Shahrul, K.; Alemu, L.T. Numerical investigation of API 31 cyclone separator for mechanical seal piping plan for rotating machineries. *Alex. Eng. J.* **2022**, *61*, 1597–1606. [[Google Scholar](#)] [[CrossRef](#)]
58. Werther, J.; Reppenhagen, J. Catalyst Attrition in Fluidized-Bed Systems. *AIChE J.* **1999**, *45*, 2001–2010. [[Google Scholar](#)] [[CrossRef](#)]
59. Werther, J.; Xi, W. Jet attrition of catalyst particles in gas fluidized beds. *Powder Technol.* **1993**, *76*, 39–46. [[Google Scholar](#)] [[CrossRef](#)]
60. Reppenhagen, J.; Werther, J. Catalyst attrition in cyclones. *Powder Technol.* **2000**, *113*, 55–69. [[Google Scholar](#)] [[CrossRef](#)]
61. Werther, J.; Reppenhagen, J. Attrition. In *Handbook of Fluidization and Fluid-Particle Systems*; Yang, W., Ed.; CRC Press: Boca Raton, FL, USA, 2003. [[Google Scholar](#)]
62. Ghadiri, M.; Cleaver, J.A.S.; Tuponogov, V.G.; Werther, J. Attrition of FCC powder in the jetting region of a fluidized bed. *Powder Technol.* **1994**, *80*, 175–178. [[Google Scholar](#)] [[CrossRef](#)]
63. Haig, C.W.; Hursthouse, A.; McIlwain, S.; Sykes, D. The effect of particle agglomeration and attrition on the separation efficiency of a Stairmand cyclone. *Powder Technol.* **2014**, *258*, 110–124. [[Google Scholar](#)] [[CrossRef](#)]
64. Griffiths, W.D.; Boysan, F. Computational fluid dynamics (CFD) and empirical modelling of the performance of a number of cyclone samplers. *J. Aerosol Sci.* **1996**, *27*, 281–304. [[Google Scholar](#)] [[CrossRef](#)]
65. Gimbun, J.; Chuah, T.G.; Choong, T.S.Y.; Fakhru'l-Razi, A. A CFD study on the prediction of cyclone collection efficiency. *Int. J. Comp. Meth-Sing.* **2005**, *6*, 161–168. [[Google Scholar](#)] [[CrossRef](#)]
66. Gimbun, J.; Chuah, T.G.; Fakhru'l-Razi, A.; Choong, T.S.Y. The influence of temperature and inlet velocity on cyclone pressure drop: A CFD study. *Chem. Eng. Process* **2005**, *44*, 7–12. [[Google Scholar](#)] [[CrossRef](#)]
67. Elsayed, K.; Lacor, C. Optimization of the cyclone separator geometry for minimum pressure drop using mathematical models and CFD simulations. *Chem. Eng. Sci.* **2010**, *65*, 6048–6058. [[Google Scholar](#)] [[CrossRef](#)]
68. Park, D.; Go, S.J. Design of Cyclone Separator Critical Diameter Model Based on Machine Learning and CFD. *Processes* **2020**, *8*, 1521. [[Google Scholar](#)] [[CrossRef](#)]
69. Hoekstra, A.J.; Derksen, J.J.; Van, H.E.A.; Akker, D. An experimental and numerical study of turbulent swirling flow in gas cyclones. *Chem. Eng. Sci.* **1999**, *54*, 2055–2065. [[Google Scholar](#)] [[CrossRef](#)] [[Green Version](#)]
70. Slack, M.D.; Prasad, R.O.; Bakker, A.; Boysan, F. Advances in cyclone modelling using unstructured grids. *Chem. Eng. Res. Des.* **2000**, *78*, 1098–1104. [[Google Scholar](#)] [[CrossRef](#)]
71. Gronald, G.; Derksen, J.J. Simulating turbulent swirling flow in a gas cyclone: A comparison of various modeling approaches. *Powder Technol.* **2011**, *205*, 160–171. [[Google Scholar](#)] [[CrossRef](#)]
72. Alexander, R.M. Fundamentals of cyclone design and operation. *Proc. Aust. Inst. Miner. Met.* **1949**, *152*, 152–153. [[Google Scholar](#)]
73. Gimbun, J.; Chuah, T.G.; Choong, T.S.Y.; Fakhru'l-Razi, A. Prediction of the effects of cone tip diameter on the cyclone performance. *J. Aerosol Sci.* **2005**, *36*, 1056–1065. [[Google Scholar](#)] [[CrossRef](#)]

74. El-Emam, M.A.; Zhou, L.; Shi, W.; Chen, H. Performance evaluation of standard cyclone separators by using CFD-DEM simulation with realistic bio-particulate matter. *Powder Technol.* **2021**, *385*, 357–374. [[Google Scholar](#)] [[CrossRef](#)]
75. Li, H.; Wang, L.; Du, C.; Hong, W. CFD-DEM investigation into flow characteristics in mixed pulsed fluidized bed under electrostatic effects. *Particuology* **2021**, *65*, 1–38. [[Google Scholar](#)] [[CrossRef](#)]
76. Nakhaei, M.; Lu, B.; Tian, Y.; Wang, W.; Kim, D.-J.; Wu, H. CFD Modeling of Gas–Solid Cyclone Separators at Ambient and Elevated Temperatures. *Processes* **2019**, *8*, 228. [[Google Scholar](#)] [[CrossRef](#)] [[Green Version](#)]
77. Li, Z.; Tong, Z.; Yu, A.; Miao, H.; Chu, K.; Zhang, H.; Guo, G.; Chen, J. Numerical investigation of separation efficiency of the cyclone with supercritical fluid-solid flow. *Particuology* **2022**, *62*, 36–46. [[Google Scholar](#)] [[CrossRef](#)]
78. Hamed, S.; Mohammad, R.; Dariush, A. Numerical study of flow field in new design cyclones with different wall temperature profiles: Comparison with conventional ones. *Adv. Powder Technol.* **2021**, *32*, 3268–3277. [[Google Scholar](#)] [[CrossRef](#)]
79. Chen, J.; Jiang, Z.; Yang, B.; Wang, Y.; Zeg, F. Effect of inlet area on the performance of a two-stage cyclone separator. *Chin. J. Chem. Eng.* **2021**, *36*, 1–35. [[Google Scholar](#)] [[CrossRef](#)]
80. Zhang, Z.; Dong, S.; Dong, K.; Hou, L.; Wang, W.; Wei, Y.; Wang, B. Experimental and numerical study of a gas cyclone with a central filter. *Particuology* **2021**, *65*, 1–46. [[Google Scholar](#)] [[CrossRef](#)]
81. Mazyan, W.I.; Ahmadi, A.; Brinkerhoff, J.; Ahmed, H.; Hoorfar, M. Enhancement of cyclone solid particle separation performance based on geometrical modification: Numerical analysis. *Sep. Purif. Technol.* **2018**, *191*, 276–285. [[Google Scholar](#)] [[CrossRef](#)]
82. Reddy Karri, S.B.; Ray, C.; Knowlton, T. Erosion in Second Stage Cyclones: Effects of Cyclone Length and Outlet Gas Velocity. In Proceedings of the 10th International Conference on Circulating Fluidized Beds and Fluidization Technology-CFB-10, Sun River, OR, USA, 1–5 May 2013; Available online: <http://dc.engconfintl.org/cfb10/40> (accessed on 5 October 2022).
83. Peukert, W.; Wadenpohl, C. Industrial separation of fine particles with difficult dust properties. *Powder Technol.* **2001**, *118*, 136–148. [[Google Scholar](#)] [[CrossRef](#)] [[Green Version](#)]
84. Salakhova, E.I.; Dmitriev, A.V.; Zinurov, V.E.; Nabiullin, I.R.; Salakhov, I.I. Dust Collector for Paraffin Dehydrogenation Units with a Fluidized Catalyst Bed. *Catal. Ind.* **2022**, *14*, 369–375. [[Google Scholar](#)] [[CrossRef](#)]
85. Zinurov, V.E.; Dmitriev, A.V.; Kharkov, V.V. Design of High-Efficiency Device for Gas Cleaning from Fine Solid Particles. In Proceedings of the 6th International Conference on Industrial Engineering, Delhi, India, 18–19 June 2021; pp. 378–385. [[Google Scholar](#)] [[CrossRef](#)]
86. Lim, J.-H.; Oh, S.-H.; Kang, S.; Lee, K.-J.; Yook, S.-J. Development of cutoff size adjustable omnidirectional inlet cyclone separator. *Sep. Purif. Technol.* **2021**, *276*, 1–9. [[Google Scholar](#)] [[CrossRef](#)]
87. Salakhova, E. I., Zinurov, V. E., Dmitriev, A., & Salakhov, I. I. (2023). Modeling of Erosion in a Cyclone and a Novel Separator with Arc-Shaped Elements. *Processes*, *11*(1), 156. <https://doi.org/10.3390/pr11010156>
88. Total Energy. Available online: <https://www.eia.gov/totalenergy/data/browser> (accessed on 30 December 2021).
89. Conti, J.; Holtberg, P.; Diefenderfer, J.; LaRose, A.; Turnure, J.T.; Westfall, L. *International Energy Outlook 2016 with Projections to 2040*; USDOE Energy Information Administration (EIA): Washington, DC, USA, 2016.
90. Energy. Our World in Data. 2015. Available online: <https://ourworldindata.org/energy> (accessed on 24 April 2019).
91. Bunse, K.; Vodicka, M.; Schönsleben, P.; Brühlhart, M.; Ernst, F.O. Integrating energy efficiency performance in production management–gap analysis between industrial needs and scientific literature. *J. Clean. Prod.* **2011**, *19*, 667–679. [[Google Scholar](#)] [[CrossRef](#)]



92. Kaya, D.; Phelan, P.; Chau, D.; Sarac, H.I. Energy conservation in compressed-air systems. *Int. J. Energy Res.* **2002**, *26*, 837–849. [[Google Scholar](#)] [[CrossRef](#)]
93. Close, C.M.; Frederick, D.K.; Newell, J.C. *Modeling and Analysis of Dynamic Systems*; John Wiley & Sons Inc.: New York, NY, USA, 2002; p. 576. [[Google Scholar](#)]
94. Naidu, D.S.; Rieger, C.G. Advanced control strategies for heating, ventilation, air-conditioning, and refrigeration systems—An overview: Part I: Hard control. *HVAC&R Res.* **2011**, *17*, 2–21. [[Google Scholar](#)]
95. Naidu, D.S.; Rieger, C.G. Advanced control strategies for HVAC&R systems—An overview: Part II: Soft and fusion control. *HVAC&R Res.* **2011**, *17*, 144–158. [[Google Scholar](#)]
96. Clarke, K.L.; Pugsley, T.; Hill, G.A. Fluidization of moist sawdust in binary particle systems in a gas–solid fluidized bed. *Chem. Eng. Sci.* **2005**, *60*, 6909–6918. [[Google Scholar](#)] [[CrossRef](#)]
97. Kunii, D.; Levenspiel, O. *Fluidization Engineering*, 2nd ed.; Butterworth-Heinemann: Stoneham, MA, USA, 1991. [[Google Scholar](#)]
98. Leith, D.; Mehta, D. Cyclone performance and design. *Atmos. Environ.* **1973**, *7*, 527–549. [[Google Scholar](#)] [[CrossRef](#)]
99. Huang, A.-N.; Ito, K.; Fukasawa, T.; Fukui, K.; Kuo, H.-P. Effects of particle mass loading on the hydrodynamics and separation efficiency of a cyclone separator. *J. Taiwan Inst. Chem. Eng.* **2018**, *90*, 61–67. [[Google Scholar](#)] [[CrossRef](#)]
100. Gomes, L.M.; Mesquita, A.L. On the prediction of pickup and saltation velocities in pneumatic conveying. *Braz. J. Chem. Eng.* **2014**, *31*, 35–46. [[Google Scholar](#)] [[CrossRef](#)][[Green Version](#)]
101. Beulac, P., Issa, M., Ilinca, A., & Brousseau, J. (2022). Parameters Affecting dust collector Efficiency for Pneumatic conveying: a review. *Energies*, *15*(3), 916. <https://doi.org/10.3390/en15030916>
102. Zhang, J., Liang, D., & Cao, Y. (2023). Analysis of dust reduction characteristics of multistage tandem dust removal system. *Shock and Vibration*, *2023*, 1–11. <https://doi.org/10.1155/2023/5541196>
- 103.

